Journal of The Electrochemical Society, **165** (5) E208-E213 (2018)
0013-4651/2018/165(5)/E208/6/$37.00 © The Electrochemical Society

Fabrication of Nano-Structured Stacked Sphere SnO_2-Sb Electrode with Enhanced Performance Using a Situ Solvothermal Synthesis Method

Lisha Yang,[1] Junfeng Liu,[1] Linlin Huang,[1] Zhaohan Zhang,[1] Yanling Yu,[1] Jia Liu,[1] Bruce E. Logan,[1,2,z] and Yujie Feng [1,z]

[1]*State Key Laboratory of Urban Water Resource & Environment, School of Environment, Harbin Institute of Technology, Harbin 150090, People's Republic of China*
[2]*Department of Civil and Environmental Engineering, The Pennsylvania State University, University Park, Pennsylvania 16802, USA*

A titanium-base nano-coating Sb-doped SnO_2 electrode with a nano-scaled sphere-stacking structure was successfully fabricated using a solvothermal synthesis approach to enhance electrochemical performance through the formation of a nano-sized catalyst layer. Based on scanning electron microscopy (SEM) and X-ray diffraction (XRD) analysis, the nano-coated SnO_2-Sb electrode had very small (23 nm) catalyst grains that had a stacked sphere appearance, and thus a much greater specific surface area than the control electrode (SnO_2-Sb prepared by a dip-coating method, 106 nm grain size). X-ray photoelectron spectroscopy (XPS) analysis showed that the nano-coated electrode possessed a higher concentration of oxygen vacancies, which provided many more active centers for the formation of adsorbed Oxygen (Oads), which increased the production of •OH radicals and therefore the catalytic activity of organic pollutant degradation. Linear sweep voltammetry (LSV) and electrochemical impedance spectroscopy (EIS) showed that the electrode with a nano-structure coating had a higher oxygen evolution potential (2.1 V, vs. Ag/AgCl) and smaller charge transfer resistance (49 Ω) than the control (1.95 V and 93 Ω). A kinetic analysis of the electrochemical degradation of phenol showed that the first-order kinetic rate constant for the nano-coated electrode was 1.72 times higher than the control. Accelerated service life testing showed that the stability of this novel fabricated electrode was 15 h, which was nearly 11 times longer than that of non-nano SnO_2-Sb electrode.
 [DOI: 10.1149/2.0711805jes]

Manuscript submitted January 23, 2018; revised manuscript received March 8, 2018. Published March 31, 2018.

Advanced oxidation processes (AOPs) are being investigated as methods to degrade or increase the biodegradability of dissolved organic pollutants that are resistant to biological degradation. These AOPs are used to generate hydroxyl radicals (•OH), which are strong oxidizing agents of the organic matter.[1–3] Among different types of AOPs, the most common one is the electrocatalytic (EC) or anodic (AO) oxidation process, due to its advantages of high effectiveness, fast reaction rates, easy implementation, and environmental compatibility.[4–8] In the EC process, pollutants are oxidized by direct charge transfer at the surface of the anode, or by indirect oxidation via production of intermediates of the oxygen evolution reaction such as hydroxyl radicals.[9,10]

The most important factor in the extent of organic compounds mineralization by EC is the anode material, as its chemical and physical nature strongly influences the selectivity and efficiency of the process.[11,12] Certain types of anodes are better for partial or selective oxidation of pollutants (i.e., electrochemical conversion), while others are more useful for complete oxidation to CO_2 (i.e., electrochemical incineration, ECI).[13–15] For this reason, numerous anodic materials have been examined, including Pt, graphite, boron-doped diamond (BDD), and dimensionally stable anodes (DSA) that consist of Ti-based metal coated oxides such as IrO_2, RuO_2, PbO_2 and Sb-SnO_2.[16,17] Among these different materials, those are made of, or contain, Sb-doped SnO_2 are considered to be superior for the ECI process due to their low cost, easy preparation, high oxygen evolution potential, and efficiency for the removal of organic contaminants.[18–22]

Increasing the he specific surface area of the metallic oxide in the Sb-SnO_2 coating can improve performance. Therefore, development of a higher specific area coating at the nanoscale should provide more active sites for the electrocatalysis oxidation reaction, and enhance electrocatalytic activities.[23–25] The grain size of a catalytic coating depends on the preparation method of the electrode. A number of methods have been used for the synthesis of nano-sized metallic oxides, including sol-gel processes,[26] electrodeposition,[27] plasma chemical vapor deposition (PCVD),[28] and magnetron sputtering.[29] The sol-gel process is one of the most widely used methods, but it uses a coating procedure that must be repeated several times, and thus electrode fabrication requires a long time in order to obtain a seeding layer with good coverage. Other methods, like PCVD and sputtering processes, require sophisticated equipment that may not be widely accessible, or that are too difficult to use for large-scale production of electrodes. Solvothermal synthesis is an alternative approach to produce a nanoparticle layer on different substrates, and it is simple and more environmentally friendly procedure than other methods. For solvothermal synthesis, the nano-scaled metal oxide layer can be formed in situ under certain temperatures and pressures provided by the hydrothermal environment, and it can easily be used for large-scale synthesis of uniform and continuous catalytic layers on the electrode substrate.[30–32]

In the present work, a sphere-stacking nano-structure SnO_2-Sb electrode was fabricated using an in situ solvothermal synthesis method, and the mechanism of enhanced electrochemical performance was examined using different electrochemical techniques. The optimal preparation condition was determined by a series of chemical (phenol) degradation tests and by using XRD analysis. The key factors impacting the performance of the nano-structured electrode were determined by comparing its performance to a control SnO_2-Sb electrode that was prepared by a dip coating method, and therefore the control lacked nano-sized particles.

Materials and Methods

Preparation of Ti-based Sb-doped SnO_2 electrode.—Ti foils (0.5 mm thick, 99.6% purity) were mechanically polished and rinsed with distilled water in an ultrasonic cleaner several times, and degreased with acetone. They were then etched in 10% oxalic acid at 98°C for 2 h, and rinsed thoroughly with deionized water. The precursor solution was freshly prepared by dissolving $SnCl_4 \cdot 5H_2O$ and $SbCl_3$ in a mixture of ethanol and concentrated hydrochloric acid, with a Sn:Sb molar ratio of 10:1. The precursor solution concentration was varied from 0.05 mol L^{-1} to 0.5 mol L^{-1} of Sn. The treated Ti substrate was fixed with a Teflon holder, placed vertically in a Teflon-lined stainless steel autoclave, and the solvothermal reaction was conducted in the autoclave (with the reactor sealed in the end) at 180°C for 6 h∼14 h with mixing using a magnetic stir bar. The solution was then drained and the resulting Ti substrate was rinsed

[z]E-mail: yujief@hit.edu.cn; bel3@engr.psu.edu

carefully with deionized water. The electrode was air-dried and crystallized by annealing in an air atmosphere in an oven, at temperatures ranging from 400°C to 600°C, for times ranging from 0.5 h to 3 h.

For comparison, Sb-doped SnO_2 electrode (control, no nanocoating) was prepared by the dip-coating method.[11] The pretreated Ti sheet was placed in 100 mL of isopropanol solution containing 17.5 g $SnCl_4 \cdot 5H_2O$, 0.87 g Sb_2O_3 and 3 mL of concentrated (37%) HCl for 30 s, dried at 90°C for 15 min, and then baked at 500°C for 10 min. This procedure was repeated 15 times, and then the electrode was annealed in a muffle oven under air flow for 1 h at a temperature of 600°C.

Characterization of electrodes.—The surface morphologies of the electrodes were analyzed using a field-emission scanning electron microscopy (SEM, S-4700, Hitachi Ltd, Japan). The crystal structure of the electrode was analyzed by X-ray diffraction (XRD, D8 ADVANCE, Germany) with Cu K_α radiation (0.154 nm). The crystal size of SnO_2-Sb particles was calculated according to Scherrer formula: $D = K\lambda/(\beta\cos\theta)$, where D is the crystallite size, K is the Scherrer constant (0.89), λ is the wavelength of incident ray, β is the full width at half maximum of the peak, and θ is the position of plane peak.[33] The chemical states of the elements on the surface of the coating were studied using X-ray photoelectron spectroscopy (XPS, PHI 5700 ESCA System, America) with Al K_α radiation ($h\upsilon = 1486.6$ eV). The percentages of different species in the samples were calculated based on XPS intensities and sensitivities (XPSPAKE41). The loading amounts of SnO_2-Sb electrodes prepared by different methods were measured by weighing the electrode substrate before and after the SnO_2-Sb deposition process using a balance.

Electrochemical analysis methods.—An electrochemical workstation (Auto Lab PGSTAT128N, Metrohm, Swiss) was used for all electrochemical studies. The as-prepared Ti-based Sb-doped SnO_2 electrodes served as the working electrode with a test area of 1×1 cm^2, with a platinum sheet (1.5×1.5 cm^2) as the counter electrode, and saturated Ag/AgCl electrode as the reference electrode. Linear sweep voltammetry (LSV) measurements were performed for the Sb-doped SnO_2 electrodes to define their oxygen evolution over-potential in a 0.5 mol L^{-1} H_2SO_4 solution at a scan rate of 1 mV s^{-1}. Electrochemical impedance spectroscopy (EIS) measurements were conducted over a range of $10^5 \sim 10^{-1}$ Hz and at a potential of 2.0 V (vs. Ag/AgCl) with an amplitude signal of 5 mV in 0.25 mol L^{-1} Na_2SO_4 solution. An equivalent circuit was used to analyze the EIS spectra.

Generation of hydroxyl radicals.—Hydroxyl radicals (•OH) produced by the SnO_2 electrodes were determined by terephthalic acid trapping and fluorescence spectroscopy (FP-6500 spectrofluorometry, Jasco Co.). The electrolyte (Na_2SO_4, 0.25 mol L^{-1}) contained 0.5 mmol L^{-1} of terephthalic acid, and was tested at a current density of 10 mA cm^{-2}. Samples (1 mL) were withdrawn from the electrochemical test chamber, diluted 50 times, and examined for fluorescence using an excitation wavelength of 315 nm and detection wavelength of 425 nm.

Electrochemical oxidation of phenol.—Phenol was chosen as the degradation probe to determine the catalytic performance of the electrodes for treatment of aromatic compounds in wastewaters. Electrochemical phenol degradation experiments were carried out in a beaker reactor with a magnetic stirrer to enhance mass transfer. The working anode had an area of 2×2 cm^2, a stainless steel with the same dimension as the cathode, and the gap between the electrodes was set as 1 cm. An 80 mL sample of 100 mg L^{-1} phenol was tested in a 0.25 mol L^{-1} Na_2SO_4 electrolyte at a current density of 10 mA cm^{-2}. Phenol concentrations were using the 4-aminoantipyrine direct spectrophotometric method with UV-Vis spectrophotometer (TU-1810, PERSEE, China). The logarithmic relationship of phenol concentration with electrolysis time was fitted to the pseudo-first-order kinetics model: $\ln(C_0/C_t) = -kt$, where C_0 is the initial concentration of phenol, C_t is the phenol's concentration at given time t, and k is the kinetic constant.

Service life test.—A service life test was used to measure the stability of the electrodes. The accelerated service life tests with the Sb-doped SnO_2 electrodes were performed in 0.5 mol L^{-1} H_2SO_4 solution under galvanostatic control at a current density of 100 mA cm^{-2}. The cell voltage was examined over time, with the service life defined as the time until the rapid increase in voltage as shown by the inflection point in the voltage curve.

Results and Discussion

Optimized conditions for the Sb-doped SnO_2 electrode prepared by the solvothermal method.—In a solvothermal synthesis process, the precursor solution concentration and solvothermal reaction time were the determinants of performance, as they were the variables impacting the formation of a uniform and compact catalytic layer. Therefore, the impacts of these two variables were examined based on their impact of phenol degradation rates. Based on the rates of phenol degradation at different precursor solution concentrations (Figure 1a), an optimal concentration of 0.1 mol L^{-1} was selected for further experiments, based on a maximum of $86.6 \pm 4.3\%$ of phenol degraded after 2 h. Variation in the solvothermal reaction times (Figure 1b) showed that the removal efficiency for SnO_2-Sb firstly increased and then decreased with the reaction time in the range of 6 h to 14 h. The fastest removal was obtained for a solvothermal reaction time of 12 h, with the highest removal of $86.6 \pm 4.3\%$.

The annealing temperatures and times had significant impacts on the electrocatalytic activity of the SnO_2-Sb electrode for phenol removal (Figures 1c and 1d). The SnO_2-Sb electrode with the heat-treatment conditions of 500°C and 1 h possessed the best electrocatalytic performance ($86.6 \pm 4.3\%$ within 2 h).

To further explore the effect of preparation parameters, the crystal structure of the SnO_2-Sb electrode was investigated by the XRD patterns (Figure 2). The peak intensity of (110) plane for the SnO_2 was enhanced with the increase in precursor solution concentration from 0.05 mol L^{-1} to 0.1 mol L^{-1} (Figure 2a), which showed that elevating concentration produced more useful crystals of SnO_2 on the substrate. However, the reflection intensity of the Ti peaks was increased when the concentration increased from 0.1 mol L^{-1} to 0.5 mol L^{-1}, demonstrating that the substrate was not evenly covered by the SnO_2 particles, which resulted in clumping if the film that formed was too thick due to very rapid formation of the film at a high precursor solution concentration. The results showed that the precursor solution concentration had significant influence on the crystallization of the SnO_2 and the coverage degree for the Ti substrate, and then on the electrocatalytic performance of the electrode.

The reflection intensity of the (110) peak for SnO_2 increased as the solvothermal reaction time was increased from 6 h to 12 h, but it did not further change when the reaction time was increased to 14 h (Figure 2b). This change peak intensity showed that increasing the reaction time was conducive to obtaining better crystals of SnO_2, but that very long times (>12 h) had little effect on the crystallization. In addition, the grain size of SnO_2-Sb electrode increased with the reaction time from 12 h (23 ± 1.1 nm) to 14 h (31 ± 1.5 nm). The smaller particle sizes increased the specific surface area, and thus provided more active sites. Due to the increased area, the SnO_2-Sb electrode prepared for 12 h had higher electrocatalytic efficiency.

The reflection intensity of the (110) peak increased with the annealing temperature in the range of 400°C~500°C, and then did not further change with higher temperatures (from 500°C to 600°C) (Figure 2c). The results indicated that the higher yield of nucleation and more complete growth of crystalline grain were obtained at 500°C, and further increasing temperature had little influence upon the crystalline forms after the complete growth of crystalline grain. In addition, the crystallite size become larger when the annealing temperature above 500°C (Table I). At 500°C, the best catalyst layer was obtained with an annealing time of 1 h, as this produced a better crystalline

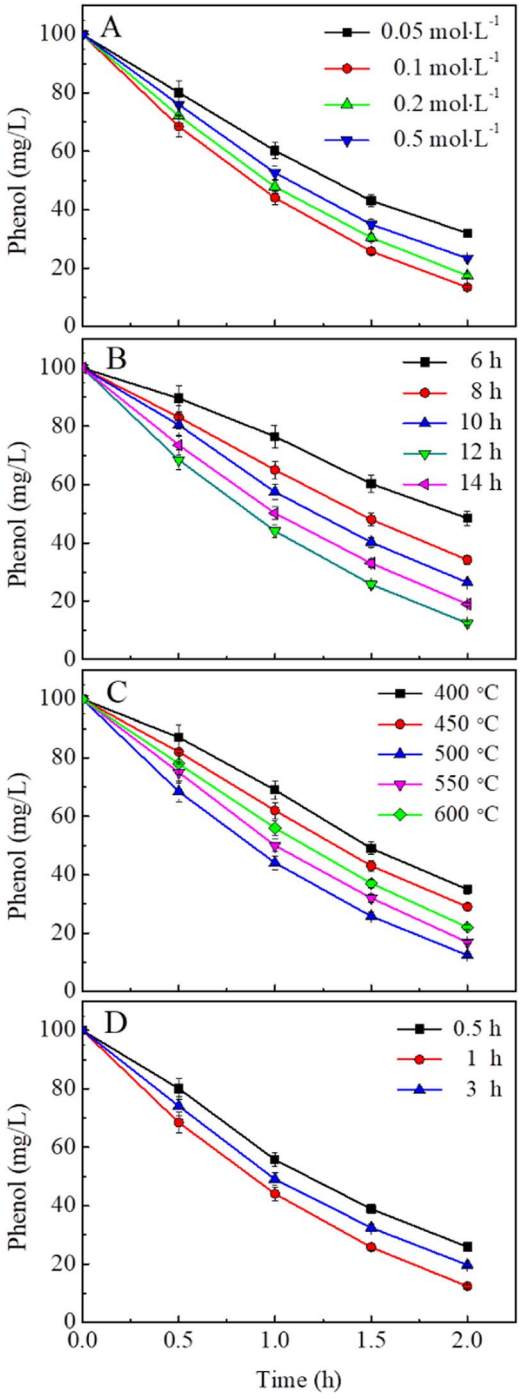

Figure 1. Effect of (A) precursor solution concentration (B) solvothermal synthesis time (C) annealing temperature and (D) annealing time of Sb-doped SnO_2 electrodes on variations of phenol concentration.

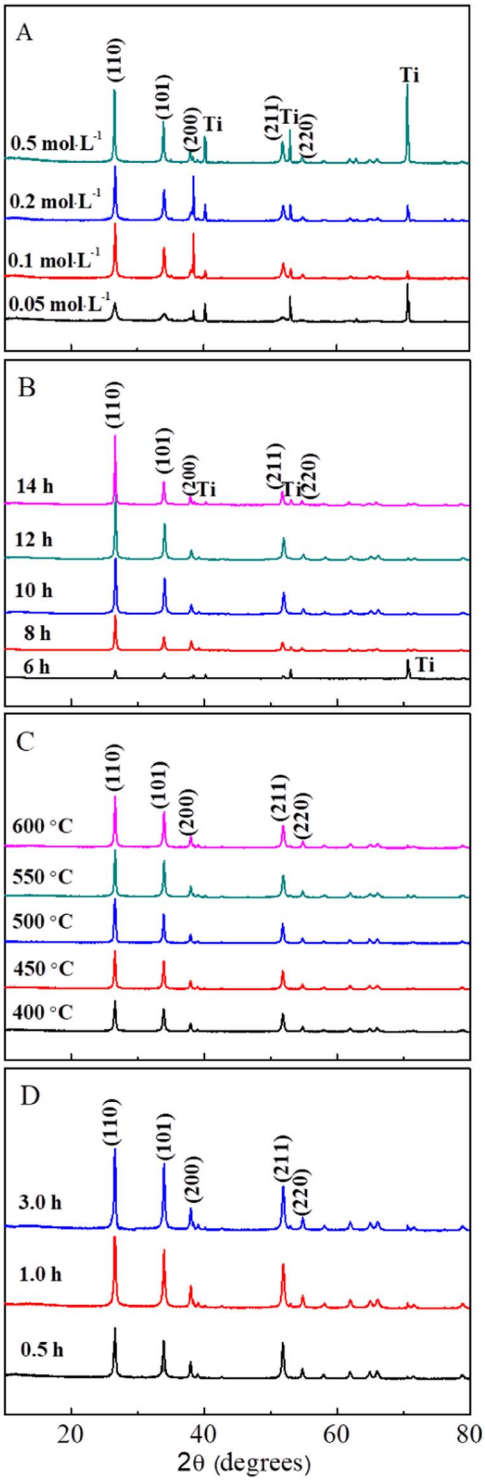

Figure 2. Effect of (A) precursor solution concentration (B) solvothermal synthesis time (C) annealing temperature and (D) annealing time on crystal structure of Sb-doped SnO_2 electrodes.

grains (compared to 0.5 h) and a smaller sizes (compared to 3 h) (Figure 2d and Table I). These outcomes suggested that annealing temperature and time affected not only crystallization but also the grain size. When the growth of crystalline grain tended to be complete, the electrode with smaller grain size could provide higher electrocatalytic oxidation efficiency, and thus the optimal annealing conditions were selected as 500°C for 1 h.

Comparison of the sno$_2$-Sb electrodes prepared by solvothermal and dip-coating methods.—The SnO_2-Sb electrode prepared by the dip-coating method was compared to the electrode prepared using the solvothermal method with the optimal conditions of 0.1 mol L^{-1} precursor solution concentration, 12 h solvothermal reaction time, and 500°C for 1 h annealing. After 2 h of treatment, phenol removal using the solvothermal SnO_2-Sb electrode was 86.6 ± 4.3%, whereas, the one by using dip-coating method was only 68.5 ± 3.4% (Figure 3a), which was similar to previous results using the dip-coating method.[12] The kinetic rate constants for phenol degradation was 16.3 × 10^{-3} min^{-1} using the solvothermal SnO_2-Sb electrode, which was

Table I. Effect of annealing conditions on the grain sizes of SnO_2.

annealing temperature (°C)	annealing time (h)	crystallite size (nm)
500	1	23 ± 1.1
500	3	27 ± 1.3
550	1	26 ± 1.3
600	1	31 ± 1.5

1.72 times that obtained using the dip-coating method electrode (9.5×10^{-3} min^{-1}) (Figure 3b). The result showed that preparation of the SnO_2-Sb electrode using the solvothermal method promoted better electrocatalytic efficiencies than the electrode made using the dip-coating method.

Electrode stability.—The SnO_2-Sb electrodes prepared by the solvothermal method had a much greater service life than the electrodes prepared using the dip-coating method (Figure 4). Initially, the potentials of the both SnO_2-Sb electrodes increased slowly. However, the potential of dip-coated electrode showed a sharp rise in voltage after only 1.4 h, indicating deactivation of electrode catalyst. In contrast, the SnO_2-Sb electrode prepared by solvothermal synthesis did not show a rapid increase in voltage for 15 h, indicating a service life that was 11 times longer than dip-coated SnO_2-Sb electrode.

Characterization analysis of the electrodes.—The load capacity on the electrode surface was strongly affected by the preparation method. The loading for SnO_2-Sb on the electrode from solvethermal method was 2.05 ± 0.02 mg cm^{-2}, which was higher than that on the electrode from dip-coating (1.87 ± 0.03 mg cm^{-2}). A high loading amount was beneficial to improve the electrocatalytic activity duo to there were more catalyst particle to attack the organic contaminant.

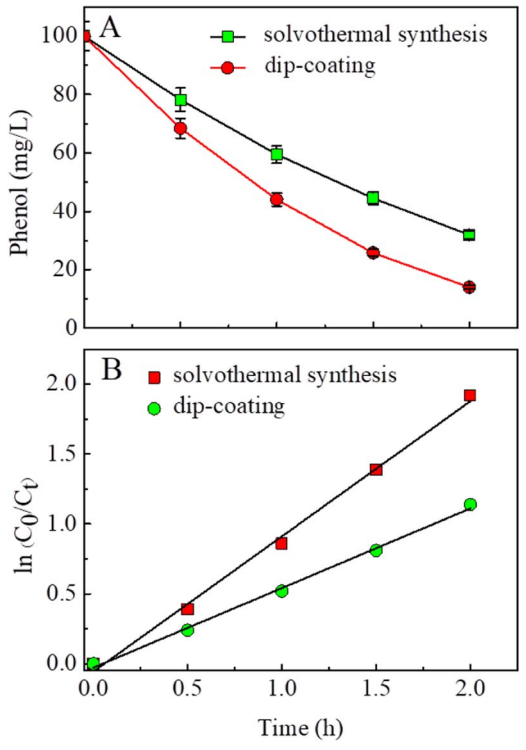

Figure 3. Electrochemical degradation of phenol on SnO_2-Sb electrodes prepared by different methods: (A) Variations of concentration of phenol with electrolysis time, and (B) the first-order kinetics curves of phenol degradation.

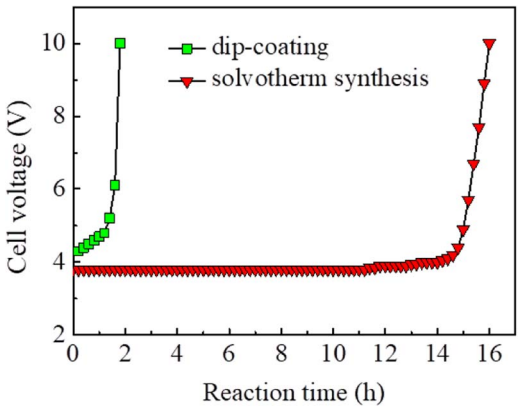

Figure 4. Variation of cell voltage in electrodes with time in accelerated life test performed in 0.5 $mol \cdot L^{-1}$ H_2SO_4 solution under 100 $mA \cdot cm^2$.

The SnO_2-Sb electrode fabricated by solvothermal synthesis method had a morphology of nano-scaled, sphere-stacking clusters (Figure 5a). In contrast, the dip-coated SnO_2-Sb electrode had a surface that showed a typical cracked surface structure (Figure 5b). The average crystal size of Sb-doped SnO_2 particles on the electrode adopted solvothermal synthesis was 23 ± 1.1 nm, which was much smaller than that of the dip-coated electrode (106 ± 5.3 nm). In addition, solvothermal synthesis method provided a better coverage on the Ti substrate, as shown by a much less intense Ti peaks ($2\theta = 39.71°$, 52.61° and 70.41°) in the XRD patterns of the solvothermal electrode than that of the dip-coated electrode (Figure 6).

Thus, the two different preparation methods produced remarkably different catalyst structures. The sphere-stacking structures obtained here also had a distinct difference with that obtained by others using the

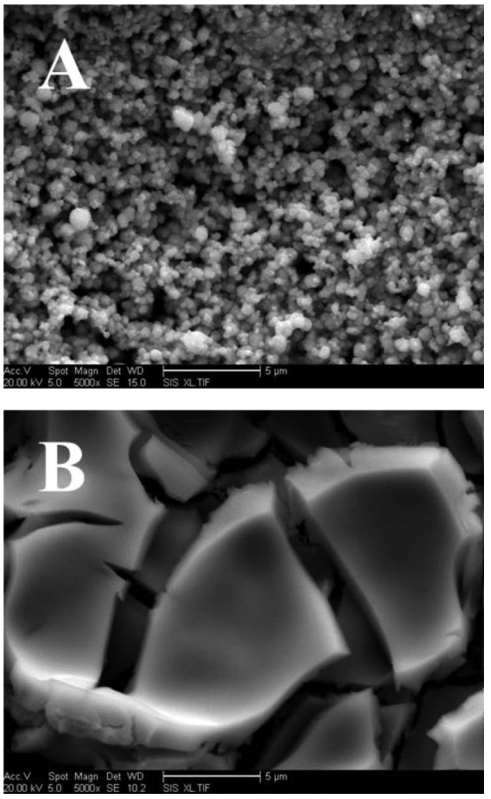

Figure 5. SEM images of SnO_2-Sb electrodes prepared by (A) solvothermal synthesis method (B) dip-coating method.

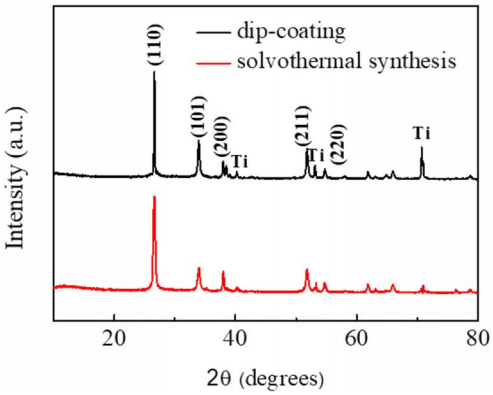

Figure 6. XRD patterns of SnO_2-Sb electrodes prepared by different methods.

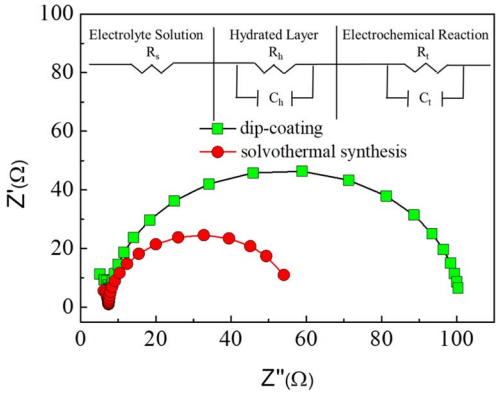

Figure 8. EIS spectra of the SnO_2-Sb electrodes prepared by different preparation methods.

solvothermal synthesis method due to synthesis process parameters having different values.[34]

Electrochemical analysis of the sno₂-Sb electrodes.—The two SnO_2-Sb electrodes fabricated by different methods had a wide potential window from 0 V to 2 V, which provided a high oxygen evolution potential of around 2 V (vs. Ag/AgCl) (Figure 7). The SnO_2-Sb electrode prepared by solvothermal synthesis method had a higher oxygen evolution potential (2.1 V vs. Ag/AgCl), as expected based on its greater efficiency for phenol degradation. The oxygen evolution potential also influences the stability of the electrode duo to the deactivation would take place by the reaction of the Ti substrate with O^{2-} ions from the reaction:

$$H_2O\,(aq) = O^{2-}\,(ox) + 2H^+\,(aq) \qquad [1]$$

A high oxygen evolution potential would result in a reduced side reaction of oxygen formation, which not only benefits organic pollutants degradation efficiency but also the service life of the electrode.

The electrochemical activity of the two SnO_2-Sb electrodes was further evaluated using EIS (Figure 8). The charge transfer resistance (Table II) for the solvothermal electrode was only 49 Ω compared to 93 Ω for the dip-coated electrode, due to the nanocoating structure and more efficient sphere-stacking clusters which provided more effective electron percolation pathways for charge transfer between interfaces of electrode and solution.

Possible mechanism of performance enhancement.—XPS analysis of the composition of the electrode surfaces indicated the increase in the adsorbed oxygen containing species would aid the generation hydroxyl radicals (•OH). (Figure 9). The Sn 3d binding energies for the two samples were around at 486.62 eV (Figure 9a), in agreement with the standard values for Sn^{4+} (486.65 eV), indicating that different morphologies did not change the valence state of Sn. The mixed spectra (Sb3d5/2 plus O1s) were fitted due to overlap in their spectra. The banding energy of Sb3d5/2 was around 530.91 eV for the two samples (Figures 9b and 9c), which was consistent with those reported in the literature for Sb^{5+}.[35]

The broadened O1s spectra were fitted into two peaks for both electrodes. The first peak at a low binding energy represented lattice oxygen (O_{lat}) which was incorporated into the SnO_2 crystal lattice. The second peak at a high binding energy was assigned to adsorbed oxygen containing species (O_{ads}), which would indicate adsorbed O_2 and/or weekly bonded oxygen species (e.g. hydroxyl group). The O_{ads} can be oxidized to hydroxyl radical (•OH), which would be effective in oxidation of organic matter, and thus this species plays an important role in the electrocatalysis oxidation process.[36] The percentage of O_{ads} contents on solvothermal electrode surface was 14.6%, which was higher than that of the dip-coated electrode (8.4%). The increased O_{ads} content was due to the high atomic concentration in the electrode's surface layer with nanometer catalyst particles, which was shown by SEM analysis (Figure 5).

The larger O_{ads} content indicated a higher concentration of oxygen vacancies was obtained on the solvothermal coated surface, which would have provided more positive charge for adsorbing hydroxyl group to form more •OH. It was therefore no surprise that the •OH generation ratio of SnO_2-Sb electrode with nano-size layer was higher than that of the one without nanocoating, as shown in Figure 9d.

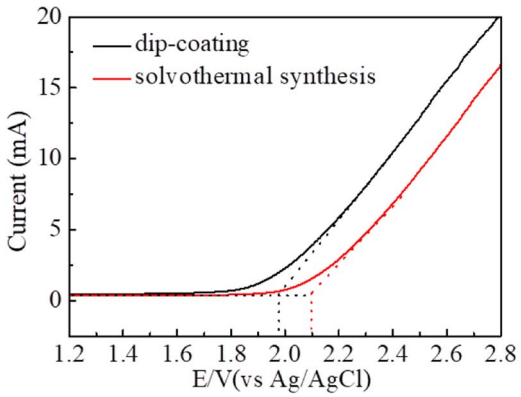

Figure 7. Polarization curves of the SnO_2-Sb electrodes prepared by different methods in the 0.5 mol·L^{-1} H_2SO_4.

Conclusions

A solvothermal synthesis method was successfully used to produce a SnO_2-Sb electrode that had superior electrochemical properties to an electrode prepared using a dip-coating methods. The optimal preparation conditions were 0.1 mol L^{-1} precursor solution concentration with synthesis time of 12 h and annealing condition of 500°C for 1 h based on phenol degradation rates. The SnO_2-Sb electrode with nanocoating had a kinetic rate constant for electrochemical phenol degradation that

Table II. EIS fitting results of SnO_2-Sb electrodes prepared by different methods.

Sample	R_s (Ω)	C_h (F)	R_h (Ω)	C_t (F)	R_t (Ω)
SnO_2-Sb (solvothermal)	4.77	6.6 E-8	33.8	2.59 E-5	49
SnO_2-Sb (dip-coating)	5.03	4.2 E-8	54.6	2.36 E-5	93

R_s represents solution resistance; C_h and R_h represent the capacitance and resistance due to the growth of a resistive hydrated layer at the oxide coating/solution interface; C_t and R_t represents the capacitance and charge transfer resistance in electrochemical oxygen evolution reaction process.

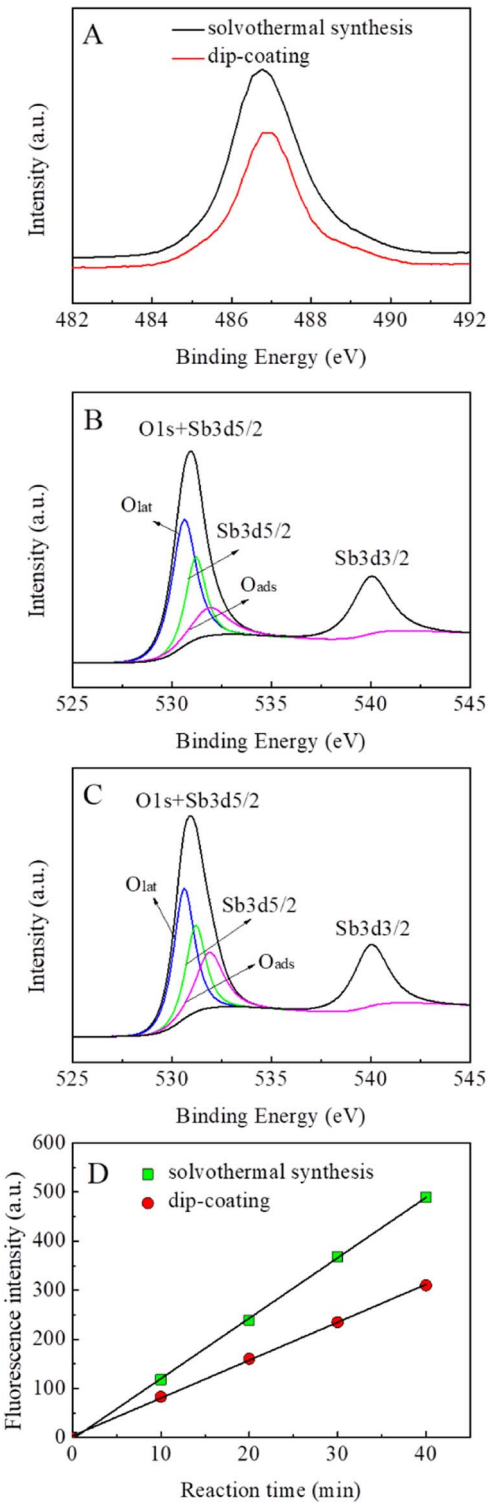

Figure 9. XPS pattern of (A) Sn3d5/2 of SnO_2-Sb electrodes, the fitted curves of O1s and Sb3d of electrodes prepared by (B) dip-coating and (C) solvothermal method, (D) hydroxyl radical generation ratio of SnO_2-Sb electrodes.

was 1.72 times that obtained for the SnO_2-Sb electrode prepared by dip coating. The service life of the nanocoated SnO_2-Sb electrode was 11 times longer than that of the dip-coated SnO_2-Sb electrode. SEM images showed that the SnO_2-Sb electrode prepared by solvothermal synthesis approach had a sphere-stacked, catalyst cluster structure due to the preparation conditions. Compared with the dip-coated SnO_2-Sb electrode, the solvothermal synthesized electrode had much smaller grain sizes and a higher concentration of oxygen vacancy sites based on the XRD and XPS analyses. This high concentration of oxygen vacancy sites provided more •OH, and therefore a higher oxygen evolution potential with 2.1 V (vs. Ag/AgCl), and a lower charge transfer resistance of 49 Ω, which all resulted in faster phenol degradation rates in the electrocatalytic process.

Acknowledgments

This work was supported by the National Key R&D Program of China (Grant No. 2016YFE0106500) and the Key Science & Technology Program of Heilongjiang Province (WB10A401). The authors also acknowledge the support of the State Key Laboratory of Urban Water Resource and Environment (Harbin Institute of Technology) (No. 2018DX01).

ORCID

Yujie Feng https://orcid.org/0000-0002-0686-3937

References

1. C. Comninellis, A. Kapalka, S. Malato, S. A. Parsons, I. Poulios, and D. Mantzavinos, *J. Chem. Technol. Biot.*, **83**, 769 (2008).
2. S. Esplugas, J. Giménez, S. Contreras, E. Pascual, and M. Rodríguez, *Water Res.*, **36**, 1034 (2002).
3. M. Pera-Titus, V. GarcíA-Molina, M. A. Baños, J. Giménez, and S. Esplugas, *Appl. Catal., B: Environ.*, **47**, 219 (2004).
4. Y. J. Feng, L. S. Yang, J. F. Liu, and B. E. Logan, Electrochemical technologies for wastewater treatment and resource reclamation *Environ. Sci.: Water Res. Technol.*, **2**, 800 (2016).
5. Y. H. Cui, Y. J. Feng, J. F. Liu, and N. Q. Ren, *J. Hazard. Mater.*, **239**, 225 (2012).
6. Y. J. Feng, Y. H. Cui, B. E. Logan, and Z. Q. Liu, *Chemosphere*. **70**, 1629 (2008).
7. J. W. Lv, Y. J. Feng, J. F. Liu, Y. P. Qu, and F. Y. Cui, *Appl. Surf. Sci.*, **283**, 900 (2013).
8. Y. J. Feng, Y. H. Cui, J. F. Liu, and B. E. Logan, *J. Hazard. Mater.*, **178**, 29 (2010).
9. D. C. Johnson and H. Chang, *J. Electrochem. Soc.*, **137**, 2452 (1990).
10. S. K. Johnson, L. L. Houk, J. R. Feng, R. S. Houk, and D. C. Johnson, *Environ. Sci. Technol.*, **33**, 2638 (1999).
11. Y. J. Feng and X. Y. Li, *Water Res.*, **37**, 2399 (2003).
12. X. Y. Li, Y. H. Cui, Y. J. Feng, Z. M. Xie, and J. D. Gu, *Water Res.*, **39**, 1972 (2005).
13. C Comninellis, *Electrochim. Acta.*, **39**, 1857 (1994).
14. C Comninellis and A. D. Battisti, *Journal de Chimie Physique et de Physico-Chimie Biologique*, **93**, 673 (1996).
15. O. Simond, V. Schaller, and C. Comninellis, *Electrochim. Acta.*, **42**, 2009 (1997).
16. M. Panizza and G. Cerisola, *Chem. Rev.*, **109**, 6541 (2009).
17. P. S. Patel, N. Bandre, A. Saraf, and J. P. Ruparelia, *Procedia Engineering*, **51**, 430 (2013).
18. T. G. Duan, Q. Wen, Y. Chen, Y. D. Zhou, and Y. Duan, *J. Hazard. Mater.*, **280**, 304 (2014).
19. Y. Duan, Q. Wen, Y. Chen, T. G. Duan, and Y. D Zhou, *Appl. Surf. Sci.*, **320**, 746 (2014).
20. Q. F. Zhuo, S. B. Deng, B. Yang, J. Huang, and G. Yu, *Environ. Sci. Technol.*, **45**, 2973 (2011).
21. L. Xu, M. Li, and W. Xu, *Electrochim. Acta.*, **166**, 64 (2015).
22. F. P Hu, X. W. Cui, and W. X. Chen, *Electrochim. Acta.*, **56**, 1576 (2011).
23. J. F. Liu, Y. J. Feng, L. X. Sun, and Z. G. Qian, Investigation on preparation and electrocatalytic characteristics of Ti-base SnO2 electrode with nano-coating. Mater. Sci. Tech., **14**, 200 (2006).
24. F. N Chianeh and J. B. Parsa, *Chem. Eng. Res. Des.*, **92**, 2740 (2014).
25. J. Q. Fan, G. H. Zhao, H. Y. Zhao, S. N. Chai, and T. C. Cao, *Electrochim. Acta.*, **94**, 21 (2013).
26. G. H. Zhao, X. Cui, M. C. Liu, P. Q. Li, Y. G. Zhang, T. C. Cao, H. X. Li, Y. Z. Lei, L. Liu, and D. M. Li, *Environ. Sci. Technol.*, **43**, 1480 (2009).
27. H. Y. Ding, Y. J. Feng, and J. F. Liu, *Mater. Lett.*, **61**, 4920 (2007).
28. K. S. Kim, S. Y. Yoon, W. J. Lee, and K. H. Kim, *Surf. Coat. Tech.*, **138**, 229 (2001).
29. S. U. Lee, W. S. Choi, and B. Hong, *Phys. Scripta.*, **129**, 312 (2007).
30. A. S. Huang, Y. S. Lin, and W. S. Yang, *J. Membrane Sci.*, **245**, 41 (2004).
31. H. Xu, Q. Zhang, W. Yan, and W. Chu, A Composite Sb-doped SnO2 Electrode Based on the TiO2 Nanotubes Prepared by Hydrothermal Synthesis. *Int. J. Electrochem. Sci.*, **6**, 6639 (2011).
32. Y. Guo, T. G. Duan, Y. Chen, and Q. Wen, *Ceram. Int.*, **41**, 8723 (2015).
33. X. Cui, G. H. Zhao, Y. Z. Lei, H. X. Li, P. Q. Li, and M. C. Liu., *Mater. Chem. Phys.*, **113**, 314 (2009).
34. A. Oury, A. Kirchev, and Y. Bultel, *Electrochim. Acta.*, **63**, 28 (2012).
35. B. Correalozano, C. Comninellis, and A. D. Battisti, *J. Electrochem. Soc.*, **143**, 203 (1996).
36. Y. H. Cui, Y. J. Feng, and Z. Q. Liu, *Electrochim. Acta.*, **54**, 4903 (2009).